Ab initio studies of borazine and benzene cyclacenes

ARTICLE *in* DIAMOND AND RELATED MATERIALS · MARCH 2003

Impact Factor: 1.92 · DOI: 10.1016/S0925-9635(03)00026-8

Available online at www.sciencedirect.com
SCIENCE DIRECT®
Diamond and Related Materials 12 (2003) 1194–1200
DIAMOND AND RELATED MATERIALS
www.elsevier.com/locate/diamond

Ab initio studies of borazine and benzene cyclacenes

S.W. Yang[a,b], H. Zhang[a], J.M. Soon[a], C.W. Lim[a], P. Wu[b], Kian Ping Loh[a,*]

[a]*Department of Chemistry, National University of Singapore, 3 Science Drive 3, Singapore*
[b]*Institute of High Performance Computing, Singapore*

Abstract

Can the borazine cyclacene system provide a conceptual framework for the investigation of the properties of hexagonal BN materials? We perform both Hartree–Fock (HF) and unrestricted density functional theory calculations for the borazine and benzene cyclacenes system to obtain insights into the structural and electronic properties as a function of the number of rings present in cyclacene. The properties of the borazine cyclacene show little dependence on the number of rings ($R \sim 4$–12) in the peripheral circuits, in contrast to the benzene cyclacene system. The frontier HOMO–LUMO gap in borazine cyclacene increases steadily with R and stabilizes at ~ 6.7 eV for $R > 9$, in contrast to the benzene cyclacene system where the gap decreases and approaches that of the semiconducting carbon nanotube system (~ 1.13 eV) for $R > 8$. The aromaticity of the rings is investigated by examining the energy separations in the frontier molecular orbitals. Vibrational modes in the borazine cyclacene systems were also calculated using HF method (HF/3-21G) and compared with experimental Raman measurements on hexagonal BN materials.

Keywords: Ab initio calculations; Borazine; Boron nitride; Cyclacene; Raman

1. Introduction

Cyclacene, a class of laterally fused benzoid hydrocarbons, offer a simple conceptual framework for understanding the structure and properties of nanotube or fullerene systems because of their remarkable similarity to these structures. A cyclacene structure can be considered as consisting of two types of embedded structures, an arenoid belt which is composed of benzenoid rings in the case of simple cyclacene, and annulenic peripheral rings which becomes either $4k$ or $4k+2$ type depending on the number of arenoid rings present. Theoretical studies of cyclacenes have shown that some properties depend strongly on the number of electrons in the peripheral circuits or the number of benzenoid rings in the arenoid belt, this effect is known as 'cryptoannulenic effect' [1–8]. Borazine is the inorganic analog of benzene, obtained by replacing each carbon with alternating boron and nitrogen atom. When borazine is folded in the same way as benzene in cyclacene, borazine cyclacene $[(BN)_n]$, where n represent the number of borazine rings will be formed. It is reasonable to consider $(BN)_n$ as the possible precursors to BN nanotubes, or BN fullerenes. BN cyclacene may exhibit interesting host–guest chemistry when metal atoms are trapped in their cylindrical cavities. There has been very little study on the borazine cyclacene system. Work on borazine cyclacene is restricted to that of Erkoc [1], in which the semiempirical method, AM1-RHF, is used and the trend towards the formation of larger BN cyclacene ring is predicted to be exothermic. The major disadvantage of semiempirical method or Hartree–Fock (HF) theory is its neglect of instantaneous electron correlation, and therefore it is not accurate enough to describe electronic properties of systems considered. In an effort to compute molecular properties more accurately by including electron correlation, density functional theory (DFT) is the method of choice in this study. In this work, we look closely at the molecular and electronic structure to understand whether aromatic stabilization and cryptoannulenic effect exists in the borazene cyclacene systems. The Raman frequencies are calculated as a function of ring size to see if the phonon vibrations of the cyclacene system agrees with experimental surface enhanced Raman study of hexagonal BN materials.

*Corresponding author. Fax: +65-67791691.
E-mail address: chmlohkp@nus.edu.sg (K.P. Loh).

0925-9635/03/$ - see front matter © 2003 Elsevier Science B.V. All rights reserved.
PII: S0925-9635(03)00026-8

Table 1a
Structural Parameters of $(BN)_n$ [UB3LYP/6-31G(d)].

n	Point group	Dipole. M. (debye)	d_1 (Å)	d_2 (Å)	d_3 (Å)	d_4 (Å)	d_5 (Å)	α <BNB	β <NBN
4	C_{4v}	4.528	1.108	1.472	1.457	1.473	1.192	99.8	115.1
5	C_{5v}	6.015	1.016	1.459	1.457	1.460	1.192	106.4	116.5
6	C_{6v}	7.418	1.015	1.452	1.457	1.454	1.192	110.6	117.3
7	C_{7v}	8.800	1.015	1.448	1.457	1.451	1.192	115.1	117.9
8	C_{8v}	10.199	1.015	1.446	1.457	1.449	1.193	115.1	118.3
9	C_{9v}	11.600	1.014	1.444	1.457	1.448	1.192	116.6	118.7
10	C_{10v}	13.045	1.014	1.442	1.457	1.447	1.193	117.7	118.9
11	C_{11v}	14.391	1.014	1.441	1.458	1.446	1.193	118.4	119.2
12	C_{12v}	15.785	1.014	1.440	1.458	1.446	1.193	119.1	119.4

Table 1b
Structural Parameters of $(C)_n$ [UB3LYP/6-31G(d)].

n	Point group	Dipole. M. (debye)	d_1 (Å)	d_2 (Å)	D_3 (Å)	d_4 (Å)	d_5 (Å)
4	D_{4h}	0.000	1.086	1.447	1.411	$=d_2$	$=d_1$
5	D_{5h}	0.002	1.088	1.422	1.474	$=d_2$	$=d_1$
6	D_{6h}	0.002	1.088	1.418	1.451	$=d_2$	$=d_1$
7	D_{7h}	0.002	1.088	1.413	1.471	$=d_2$	$=d_1$
8	D_{8h}	0.001	1.088	1.411	1.459	$=d_2$	$=d_1$
9	D_{9h}	0.001	1.088	1.410	1.470	$=d_2$	$=d_1$

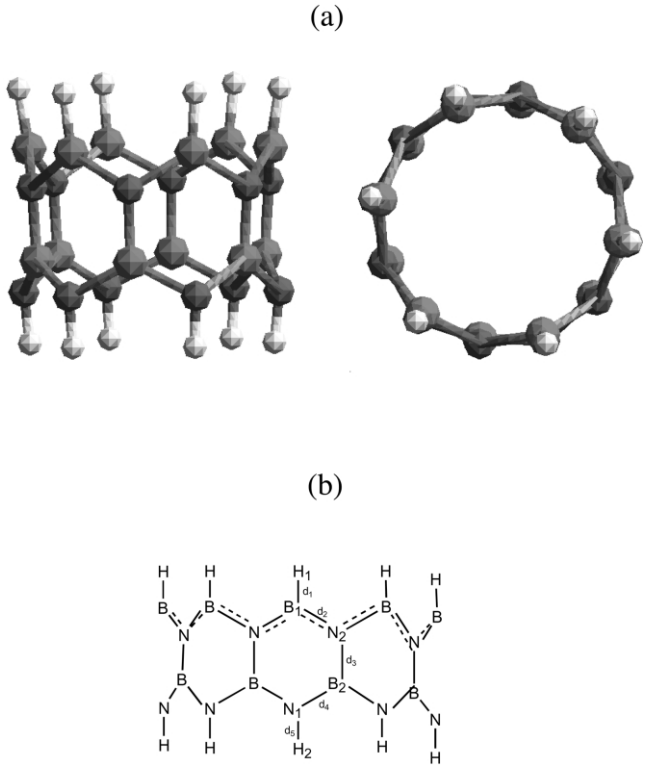

Fig. 1. (a) 3-D drawing of 6-ring borazene cyclacene, side view (left) and top view (right). A molecular analog of BN nanotube. Red, B atom; blue, N atom and grey, H atom. (b) The borazene cyclacene consisting of two transannulene-like chain coupled together. d_2, peripheral bond distances; d_3, fusion site separation.

2. Method

Two levels of calculations were carried out using Gaussian98 suite on a Sun supercomputer, E10K. Unrestricted DFT employing Becke's three parameters hybrid method and Lee-Yang-Parr's correlation correction (UB3LYP) with a 6-31G(d) basis set was applied in this work. HF method with a 3-21G basis set was also used to calculate the properties of C_n, ($n=4$–9) and $(BN)_n$ ($n=4$–12) cyclacene [9] for comparison with the DFT. Full geometry optimizations were obtained in both calculations. In addition, the Raman calculations were carried out for both systems using the HF/3-21G basis set. Experimental Raman studies on hexagonal BN (h-BN) films were carried out using the 625 nm He–Ne laser. The BN film was grown by RF-CVD using borazine as the gas feed.

3. Results and discussion

3.1. Geometry of benzene and borazine cyclacenes

The structure parameters for both C_n and $(BN)_n$ cyclacenes after full geometry optimization are listed in Tables 1a and 1b. A drawing of the cyclacene structure for $n=6$ in the case of $(BN)_6$ is shown in Fig. 1a. The symmetry of C_n is found to be D_{nh} point group from DFT calculations, which is in good agreement with the report of Choi and Kim [10]. The $(BN)_n$ have C_{nv} point group in contrast to the single molecule borazene (D_{3h}), mainly because of the loss of C_2 symmetry axis sym-

Table 2a
$(BN)_n$ optimised energy and frontier HOMO–LUMO gaps (eV)

	HF/3-21G					UB3LYP/6-31-G(d)				
n	Energy	BE	HOMO	LUMO	Δ_{gap}	Energy	BE	HOMO	LUMO	Δ_{gap}
4	−17273.47	−109.34	−8.32	0.93	10.92	−17474.27	−138.70	−5.68	−2.48	3.78
5	−21596.39	−141.23	−8.19	1.74	11.72	−21846.73	−177.27	−5.61	−1.64	4.68
6	−25918.71	−172.51	−8.45	2.38	12.77	−26218.57	−215.22	−5.76	−1.03	5.58
7	−30240.65	−203.42	−8.24	2.90	13.14	−30590.05	−252.81	−5.62	−0.57	5.96
8	−34562.37	−234.11	−8.37	3.31	13.79	−34961.33	−290.19	−5.74	−0.21	6.52
9	−38883.92	−264.63	−8.30	3.63	14.07	−39332.46	−327.44	−5.63	0.06	6.72
10	−43205.37	−295.04	−8.32	3.66	14.13	−43703.51	−364.60	−5.64	0.17	6.87
11	−47526.73	−325.37	−8.34	3.61	14.10	−48074.48	−401.68	−5.65	0.10	6.79
12	−51848.03	−355.64	−8.31	3.60	14.06	−52445.41	−438.71	−5.62	0.09	6.74

Table 2b
C_n optimised energy and frontier HOMO–LUMO gaps (eV)

	HF/3-21G					UB3LYP/6-31-G(d)				
n	Energy	BE	HOMO	LUMO	Δ_{gap}	Energy	BE	HOMO	LUMO	Δ_{gap}
4	−16506.14	−118.55	−4.92	1.73	7.85	−16710.64	−154.70	−4.15	−1.24	3.43
5	−20637.50	−153.02	−4.81	1.06	6.93	−20891.53	−196.60	−3.66	−2.08	1.87
6	−24769.18	−187.80	−3.85	−0.05	4.48	−25074.22	−240.32	−3.23	−2.18	1.24
7	−28900.94	−222.67	−4.29	0.21	5.31	−29255.88	−282.99	−3.44	−2.05	1.65
8	−33032.03	−256.86	−3.67	−0.59	3.63	−33438.04	−326.16	−3.30	−2.36	1.11
9	−37163.08	−291.02	−4.25	−0.09	4.90	−37618.77	−367.91	−3.33	−2.37	1.13

metry following the cyclization. The structure parameters obtained by DFT methods for both C_n and $(BN)_n$ after full geometry optimization are given in Tables 1a and 1b. We notice some differences between geometrical parameters obtained by the DFT methods compared to the HF methods. For C_n, all bond lengths calculated by DFT are longer than that by HF method, whereas bond angles show the reverse trend. For $(BN)_n$, all B–N bond lengths are shorter compared to that obtained by HF.

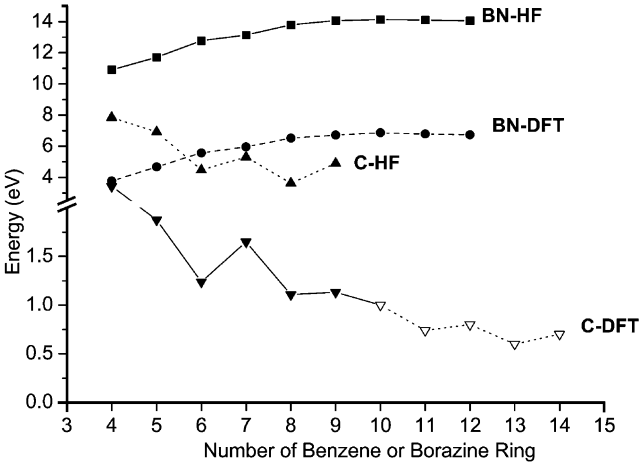

Fig. 2. Energy gaps of HOMO and LUMO for HF (HF/3-21G and DFT (UB3LYP/6-31G(d)), respectively. Broken line of C-DFT is cited from the results of Ref. [10].

Our discussion here will focus mainly on the DFT results due to its higher level of accuracy.

Fig. 1b shows a schematic of the $(BN)_n$, indicating the bonds in the peripheral sites as well as fusion sites. When compared to the molecular borazine structure (B–H = 1.011 Å and N–H = 1.197 Å, obtained with the same DFT method and basis set), the B–H bond length (r_{B-H} (d_1) = 1.015 Å) in the borazine cyclacene is longer, whilst the N–H bond length, (r_{N-H} (d_5) = 1.192 Å) is shorter. There are only slight fluctuations in these bond lengths (±0.002 Å) for B–H and N–H as a function of ring size. The $n = 4$ structure is an exception because of the high strain. The bond lengths between the fusion and peri-position, r_{N-BH} (d_2) and r_{B-NH} (d_4), decrease from 1.472 to 1.440 Å, and 1.473 to 1.446 Å, respectively, when n increases. The distance between fusion site atom (r_{B-N}) in the borazine moiety is relatively constant at 1.457 Å (±0.001 Å) and the maximum bond length alternation in d_2 and d_3 is 0.018 Å. In contrast, the r_{C-C} in the benzene moiety of cyclacene exhibits significant bond length alternation (0.03–0.06 Å) in d_2 and d_3 as n varies, as shown in Table 1b. The alternation in d_2 and d_3 suggests that the coupling between the two peripheral transannulene chain is alternatively strong and weak, a consequence of the change between the $4k$ and $4k+2$ π electrons when n alternates between odd and even. Such a change is not observed in the $(BN)_n$ system because d_3 remains effectively constant.

Table 3a
Energy levels of Frontier MOs (DFT method) in C_n (eV)

n	$\Delta_{(-1)-(0)}$	HOMO (−2)	HOMO (−1)	HOMO (0)	Δ_{gap}	LUMO (0)	LUMO (+1)	LUMO (+2)	$\Delta_{(+1)-(0)}$
4	0.80	−5.94	−5.70	−4.90	3.43	−1.47	−1.31	−1.31	0.16
5	0.00	−6.70	−4.32	−4.32	1.87	−2.45	−1.82	−1.82	0.63
6	1.70	−5.50	−5.50	−3.81	1.24	−2.57	−1.71	−1.15	0.86
7	0.00	−6.48	−4.06	−4.06	1.65	−2.41	−2.41	−1.01	0.00
8	1.07	−4.96	−4.96	−3.89	1.11	−2.79	−1.71	−1.71	1.08
9	0.00	−5.83	−3.92	−3.92	1.13	−2.79	−2.79	−0.94	0.00

$\Delta_{(-1)-(0)}$ refers to the difference in energy between $HOMO_{-1}$ and HOMO, whilst $\Delta_{(+1)-(0)}$ refers to the difference in energy between $LUMO_{+1}$ and LUMO, Δ_{gap} refers to the energy difference between HOMO and LUMO.

Table 3b
Energy levels of Frontier MOs (DFT method) in $(BN)_n$ (eV)

n	$\Delta_{(-1)-(0)}$	HOMO (−2)	HOMO (−1)	HOMO (0)	Δ_{gap}	LUMO (0)	LUMO (+1)	LUMO (+2)	$\Delta_{(+1)-(0)}$
4	0.01	−7.47	−6.70	−6.70	3.78	−2.92	−0.37	−0.17	2.55
5	0.00	−7.63	−6.62	−6.62	4.68	−1.94	−0.21	−0.20	1.73
6	0.11	−6.97	−6.91	−6.80	5.58	−1.21	−0.10	−0.09	1.11
7	0.00	−7.35	−6.63	−6.63	5.96	−0.67	0.06	0.07	0.73
8	0.00	−6.81	−6.77	−6.77	6.52	−0.25	0.23	0.23	0.48
9	0.00	−7.00	−6.65	−6.65	6.72	0.07	0.23	0.23	0.15
10	0.00	−6.78	−6.66	−6.66	6.87	0.21	0.21	0.21	0.01
11	0.00	−6.81	−6.66	−6.66	6.79	0.12	0.12	0.31	0.00
12	0.00	−6.78	−6.63	−6.63	6.74	0.11	0.11	0.12	0.00

3.2. Energy and molecular orbital

Tables 2a and 2b gives the energies and frontier molecular orbital (MO) information. Both HF and DFT calculation show that the binding energies of $(BN)_n$ increase with ring size, suggesting that it is exothermic to form bigger ring structures. Fig. 2 shows the plot of frontier HOMO–LUMO separation, Δ_{gap}, vs. n where interesting differences between the C_n and $(BN)_n$ structures can be seen. It can be seen the energy gap *increases* monotonically for $(BN)_n$ with n, but after $n=10$, the Δ_{gap} stabilizes at 6.7 eV in the DFT calculations.

In the case of C_n, both HF and DFT calculations show a decrease of the Δ_{gap} with n, such that when $n>8$, $\Delta_{gap}=1.13$ eV (DFT result), which is close to the band gap of semiconductor carbon nanotube. Interestingly, fluctuations in the Δ_{gap} value when n alternates between odd and even are seen in Table 2b. The C_n can be considered as the fusion of two [n] transannulenes. When the number of electron in the transannulene (peripheral carbon circuit) is the Hückel type ($4k+2$, n is odd), it can be seen that Δ_{gap} is higher than the immediate n value (n is even, $4k$) above and below in the column, where the number of electron in the peripheral circuit is $4k$. An example is when $n=7$, Δ_{gap} is larger than $n=6$ and $n=8$. Choi and Kim [10] indicated that when electron number is $4k$ (n is even) in the two top annulenic peripheral rings, the particular cyclacene system will tend to have two singly occupied molecular orbitals (SOMOs), so the singlet states are nonaromatic and unstable. In this case, two [$4k$] transannulene moieties tend to be coupled strongly through $r_{C–C}$ bonds, as can be judged from the somewhat short $r_{C–C}$ values. The couplings result in the alternation of the bond lengths of the fusion site (d_3) in Table 1b, with the $r_{C–C}$ value contracting whenever n is even.

The four SOMOs in the two top [$4k$] transannulene moieties when n is even are split into two occupied (HOMO and $HOMO_{-1}$) and two unoccupied MOs (LUMO and $LUMO_{+1}$), resulting in a smaller Δ_{gap}. We analyse the frontier MOs carefully for the C_n systems (Table 3a) to derive insight into the relationship between electron number in the peripheral circuit and the energy of the frontier orbitals. It is very interesting that the energy gaps between HOMO and $HOMO_{-1}$, $\Delta_{(-1)-(0)}$, alternate between zero and non-zero values when the number of electrons changes between $4k+2$ and $4k$. It is obvious that there are two types of the frontier MOs. In one case, when n is odd, the electron number is $4k+2$ and $\Delta_{(-1)-(0)}=0$, i.e. the HOMO and $HOMO_{-1}$, LUMO and $LUMO_{+1}$, are degenerate. It is observed that Δ_{gap} is higher than the case when n is even. When n is even, and electron number is $4k$, two transannulene moieties couple and generate split MOs. In this case, HOMO and $HOMO_{-1}$ are non-degenerate. The Δ_{gap}, difference between split LUMO and HOMO, is consequently smaller. A notable exception is for $n=4$, the strains are high in this system and the overlap of the p

Table 4
Typical Raman vibration frequencies (cm^{-1}) calculated by HF/3-21G

$n=4$	5	6	7	8	9	10	11	12	Vibration mode
117.2 (5.26)	108.1 (4.95)	89.6 (4.92)	71.8 (4.71)	57.2 (4.48)	46.3 (4.28)	38.2 (4.11)	31.8 (3.97)	26.3 (3.83)	Deforrmation vibration mode
161.7 (3.67)	154.4 (0.50)	130.8 (0.18)	108.1 (0.10)	89.9 (0.07)	76.3 (0.06)	65.4 (0.05)	56.3 (0.05)	49.1 (0.04)	
298.9 (4.37)	286.2 (4.03)	264.4 (5.55)	243.5 (6.59)	225.3 (7.52)	209.0 (8.34)	195.3 (9.11)	182.6 (9.84)	170.8 (10.50)	
417.9 (0.28)	364.3 (0.09)	340.7 (0.05)	313.4 (9.71)	264.4 (0.83)	257.1 (10.60)	235.3 (10.32)	215.3 (9.97)	199.0 (9.59)	Symmetry breathing mode
431.5 (1.36)	386.1 (2.83)	346.1 (6.51)	348.0 (0.09)	335.2 (0.91)	329.8 (0.08)	310.7 (0.04)	290.7 (0.02)	270.7 (0.01)	Asymmetry breathing mode
341.6 (0.39)	338.9 (5.02)	321.6 (3.59)	322.5 (0.82)	343.4 (0.11)	342.5 (0.94)	371.6 (1.65)	366.1 (1.94)	361.6 (2.11)	BH wagging vibration
674.1 (29.9)	662.3 (32.8)	659.6 (35.6)	657.8 (39.6)	657.8 (43.9)	657.8 (2.9)	656.8 (53.7)	657.8 (59.0)	656.8 (64.5)	Breathing mode (axis)

Intensity values are in bracket.

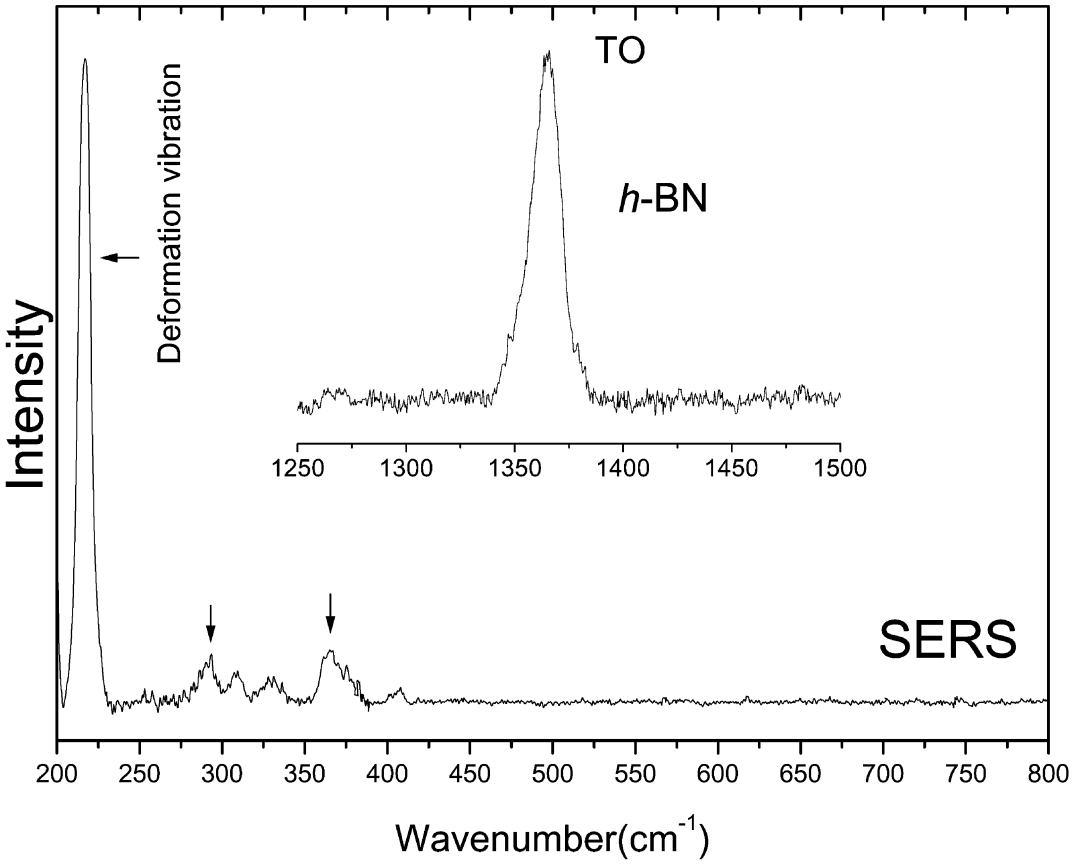

Fig. 3. Surface enhanced Raman spectrum of hexagonal BN grown on nickel, highlighting the surface phonon modes at low wavenumbers.

orbital is larger for a small system resulting in an abnormally larger $\Delta_{gap.}$

When we analyse the $(BN)_n$ frontier MO energy levels given in Table 3b, it is discovered that $\Delta_{(-1)-(0)} = 0$ for almost all systems. This implies the absence of non-degenerate HOMO and $HOMO_{-1}$, and there is no additional coupling between two top annulenic rings that arise from 'SOMO' type p orbitals. The lack of effective overlap of p orbitals, i.e. poor aromaticity, arises from the differences in electronegativity of B and N. The poor aromaticity for all values of n means that the energy gap is not affected by an alternation of the peripheral electrons between $4k$ and $4k+2$ (assuming electrons from N lone pairs). The lack of coupling did not have the effect of splitting the frontier MOs and narrowing the gap. In fact, we can see that the energy gap increases when n increases for the $(BN)_n$ systems. A tiny fluctuation can be detected in HOMO (Table 3b) so a small degree of aromaticity exists.

Generally, carbon and BN cyclacenes or nanotubes can be described as (n, m) based on the different degree of twist and fold. The C_n and $(BN)_n$ considered in the current work belong to the $(n, 0)$ class. It is known that for C_n, Δ_{gap} is very different between $(n, 0)$ and $(0, n)$ [11]. A molecular analog of this is that when benzene sheet is folded or twisted in different degree (n, m), it results in different peripheral annulene rings and new frontier MOs are generated. The change in Δ_{gap} depends sensitively on the aromaticity of the system. Our study shows that the BN systems are not sensitive to the change in the number of electrons in the peripheral circuits because the system is poorly aromatic. We can judge the poor aromaticity of the BN system from the dipole moment of $(BN)_n$ system as tabulated in Table 1a. The high dipole moment of BN cyclacene compared to the C_n system suggests that a high degree of charge separation (ionic) occurs in the former system.

3.3. Raman frequencies

Raman-active vibrational modes are calculated by HF (HF/3-21G) method. Table 4 lists some of the characteristic vibration frequencies. It is very clear that all phonon vibrations, such as deformation, symmetry and axial breathing vibrations, exhibit red shift with an increase in n. This is consistent with the increasing relaxation of the system, although the trend is not reflected in the increasing bond distances in the peripheral or fusion site atoms. The intensity of the Raman vibration is related to the ease of changing the polariz-

ability of the system in vibration. For $n<9$, the symmetric ring breathing mode is observed to have a low intensity, but increases thereafter. The asymmetric breathing mode is almost negligible for large n. This implies that as n increases, the electron clouds of the system are more readily distorted in symmetric vibration motion. The breathing mode that is parallel to the axis is almost constant at 657 cm^{-1} with n and also exhibits increasing intensity with n. The tangential breathing mode is known to be independent of the diameter of the nanotubes, as have been observed for carbon nanotubes in previous scattering study [12]. To assess whether the borazene cyclacene can be used for modeling the Raman vibrational modes in hexagonal BN systems, we perform surface enhanced Raman spectroscopy (SERS) on the hexagonal BN film in order to observe the surface phonon modes. Although the borazene cyclacene is a 'ringed' system, it is assumed that some properties may approach that of the surface phonon modes of hexagonal BN when n is large enough. Fig. 3 shows the SERS spectra obtained from crystalline hexagonal BN film, where the inset shows the transverse optical phonon of the films. The surface phonon modes due to ring breathing at 215 cm^{-1}, as well as peaks between 270 and 361 cm^{-1}, related to either asymmetry breathing or BH wagging vibration, can be observed in Fig. 3. The peak at 215 cm^{-1} is especially strong following surface enhancement. Some discrepancies in the intensities of the Raman modes may arise from the differences in symmetry between the two systems. Nevertheless for $n>10$, the borazene cyclacene system can exhibit some surface vibrational modes that are common with the surface phonon modes of the hexagonal BN system. It is interesting to consider whether the borazene cyclacene system can model the surface phonon frequencies in BN nanotubes.

4. Conclusion

We have performed ab initio studies of the carbon cyclacene and borazine cyclacene systems and analyzed the differences in aromaticities between the two systems. Fluctuations in the fusion carbon bond lengths, as well as frontier orbital energy separation, observed in the carbon cyclacene system is not observed in the borazine cyclacene system due to the poor aromaticity of the latter. The ΔE_g of the borazine cyclacene system increases with the ring size, in contrast to the carbon cyclacene system. A red shift is observed in the frequency of the borazine ring breathing modes with ring size. Some of these modes are found to agree reasonably well with the experimentally measured surface phonon modes of hexagonal BN thin films grown by CVD.

References

[1] S.J. Erkoc, Mol. Struct. (Theochem.) 540 (2001) 153–156.
[2] J.K. Parker, S.R. Davis, J. Phys. Chem. 101 (1997) 9410–9414.
[3] L. Turker, Polycycl. Aromat. Comp. 12 (1997) 213.
[4] L. Turker, J. Mol. Struct. (Theochem.) 454 (1998) 83.
[5] S.J. Erkoc, Mol. Struct. (Theochem.) 578 (2002) 99–101.
[6] L. Turker, S.J. Erkoc, Mol. Struct. (Theochem.) 531 (2001) 401–406.
[7] S.J. Erkoc, Mol. Struct. (Theochem.) 492 (1999) 159–163.
[8] L. Turker, J. Mol. Struct. (Theochem.) 531 (2000) 175–179.
[9] J.B. Foresman, E. Frisch, Exploring Chemistry with Electronic Structure Methods, Gaussian, Pittsburgh, PA, 1996.
[10] H.S. Choi, K.S. Kim, Angew. Chem. Int. Ed. 38 (15) (1999) 2256.
[11] J. McMurry, Organic Chemistry, fourth ed., Cornell University, 1996.
[12] Adv. Phys. 49 (6) (2000) 705.